

Cheng Zeng Li

Department of Electric
and Electronic
Engineering,
Technical University of
Chengdu, CHINA

Analysis and Simulation of Carrier Transport in InP-Based Double Heterojunction Photoelectronic Device

In this study, the carrier transport in InGaAs/InP double heterojunction (DHs) devices was simulated and analysed by Monte Carlo modelling. It was shown that direct modifications to the definitions of common emitter gain and base transit time re-establish the first order validity of simple analytical models of phototransistor performance based on carrier diffusion. The available evidence indicates that the correction is small, even in very narrow bases, if the base doping is high ($N_B \sim 5 \times 10^{19}$ impurities/cm³). Although the corrections to the base and c-b depletion layer transit times are large, the impact on estimates of f_t by simple theory is small owing to the dominance of RC time constants.

Keywords: Heterojunction; Phototransistors; Indium phosphide; Carrier transport
Received: 26 January 2017; **Revised:** 13 August 2017; **Accepted:** 20 August 2017

1. Introduction

Designing heterojunction transistors for applications in rf-photonics involves a trade-off between responsivity and the unity current gain frequency, f_T . Whilst edge coupling of light can ease the compromise by exploiting the waveguide properties of the heterojunction transistor structures [6], satisfying the conditions for good optical and electrical performance still requires careful optimisation of the epitaxial design. The high gain and non-linear transfer characteristics of heterojunction phototransistors offer advantages for high frequency optical receiver applications [1] and optical de-multiplexing of rf sub-carriers [2,3]. Monolithic integration of heterojunction phototransistors with heterojunction bipolar transistors has been demonstrated [4,5] and gives further incentive for establishing simple procedures for optimising heterojunction phototransistors.

A first order method has been developed for optimising edge-coupled heterojunction phototransistors [7], based on rigorous modelling of heterostructure optical waveguides [8] and earlier analytical methods for predicting optical gain [9] and f_t [10]. It assumes that carriers remain in thermal equilibrium with the lattice, a situation unlikely to occur for typical base widths in state of the art heterojunction phototransistors. Quasi-ballistic transport must be considered [11].

This paper presents new results based on detailed Monte Carlo modelling of carrier transport in double heterojunction phototransistors within the context of the earlier analytical approaches, to establish the limits on their validity for optimising device structures.

2. Heterojunction Device Design

The focus here is on optimising NPN InP/InGaAs heterojunction phototransistor layer structures for high-speed 1300 and 1550nm wavelength applications. The highest performance heterojunction phototransistors reported have a wide band gap InP sub-collector, creating a double heterostructure, with a low doped n-type InGaAs collector readily depleted by a small V_{CE} [4,5]. Figure (1) shows the basic double heterojunction phototransistor structure modelled. The InP sub-collector prevents light absorption in the neutral collector. This improves the response time by eliminating the contribution to the photocurrent from slow diffusing holes.

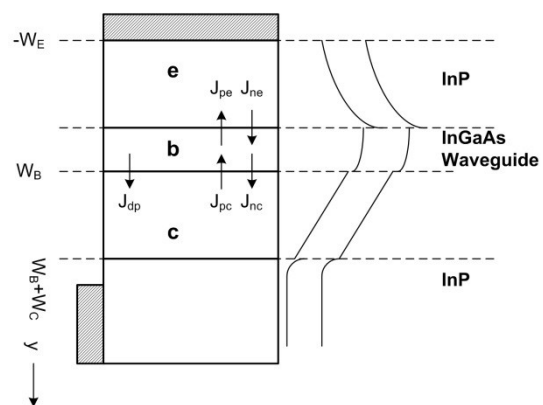


Fig. (1) Band edge variation through an edge-coupled double heterojunction phototransistor, defining base width, W_B , collector width, W_C , and contributions to output current density defined in section III

Reference [7] describes the application of a semi-vectorial finite difference (SFVD) method for solving the Helmholtz equation [8] to the double heterojunction phototransistor waveguide problem

and gives details of the refractive index values used here. The modelling included the effects of the gold contacts to the emitter and to the InP sub-collector layer, either side of the waveguide ridge. The waveguide created by mesa etching to the InP sub-collector always supported two quasi TE modes and two quasi TM modes even with the ridge width reduced to 2 μm , because of the high lateral refractive index step.

Figures (2a) and (2b) show the transverse intensity variation of the quasi-TE0 and quasi-TM0 modes supported by an edge-coupled double-heterojunction phototransistor comprising a 5 μm wide rib, with $W_E=0.15\mu\text{m}$, $W_B=0.10\mu\text{m}$ and $W_C=0.40\mu\text{m}$. This structure replicates the edge-coupled double heterojunction phototransistors reported in [1-3]. The input wavelength was 1.55 μm . The blocks either side of the waveguide represent gold collector contacts. The uppermost block represents the gold emitter contact. For TE polarisation the modes are tightly confined to the base and InGaAs collector regions, with power confinement factors of $\Gamma > 0.8$. For TM polarisation, plasmon modes are excited, owing to the proximity of the Au emitter contact to the waveguide core [7], resulting in low optical gain for this polarisation state. The TM modes acquire a guided nature with increasing W_E , as figure (2c) shows for $W_E = 0.23 \mu\text{m}$. Complete elimination of polarisation dependence in device performance requires further increases in W_E , potentially compromising f_T and the gain.

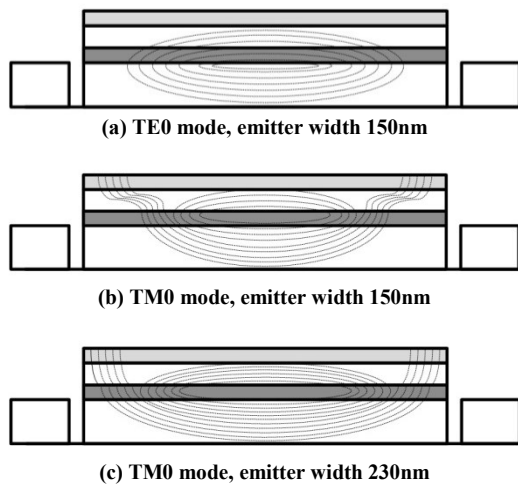


Fig. (2) Transverse intensity variation of (a) the quasi-TE0 mode, (b) quasi-TM0 mode of 5 μm wide two-terminal double heterojunction phototransistor with $W_E=0.15\mu\text{m}$, $W_B=0.10\mu\text{m}$ and $W_C=0.40\mu\text{m}$ and (c) the TMO mode with W_E to 0.23 μm

Even when the widths of the base and collector layers were reduced to 0.05 μm and 0.30 μm , respectively, the quasi-TE mode remain tightly confined to the light absorbing regions of the double heterojunction phototransistor, with their vertical intensity profile approximated by a $\{1-\cos(2\gamma y)\}$ dependence through these layers, where

$\gamma \approx \pi(W_B+W_C)$, a result exploited in developing an analytical expression for the optical gain of edge-coupled heterojunction phototransistors [7].

3. Calculations and Analysis

There are several analyses of the optical gain of heterojunction phototransistors in the literature [6,8,12] based on calculating the flux density of excess minority carriers in the base from the diffusion equation

$$D_n \frac{d^2}{dy^2} \Delta n - \frac{\Delta n}{\tau_n} + g(y) = 0 \quad (1)$$

The source term, $g(y)$, in Eq. (1) reflects the spatial variation in the photo-generation of minority carriers and contributes a term n_p to the solution. The analysis proceeds by deriving an expression for the optical bias induced on the e-b junction from the current continuity condition

$$J_{ne} - J_{pe} = J_{nc} + J_{dp} - J_{pc} \quad (2)$$

where J_{ne} (J_{pe}) is the current density of electrons (holes) across the e-b junction, J_{nc} (J_{nc}) is the current density of electrons (holes) across the c-b junction. The optical bias derives mainly from the accumulation of photo-generated holes drifting from the c-b depletion region, i.e., from drift current J_{dp} given by

$$J_{dp} = \frac{qg_0}{2} \int_{W_B}^{W_B+W_C} g(\gamma y) dy \quad (3)$$

The optical gain, G_{opt} , is found by summing all components of the collector current that originate from direct photo-generation and from the optical bias. In double heterojunction phototransistors, the following assumptions can be made: (1) the emitter efficiency is ~ 1 (equivalently $J_{pe} \approx 0$), (2) V_{CE} is large enough to deplete fully the narrow band gap collector and (3) J_{pc} has no optical component and can be neglected. For a top entry double heterojunction phototransistor, the generation term in Eq. (1) has an $e^{-\alpha y}$ dependence and, with J_{dp} dominant, the optical gain takes the form [12]

$$G_{opt,top} \approx (1 + h_{FE}) \exp(-\alpha W_B) [1 - \exp(-\alpha W_C)] \quad (4)$$

where

$$h_{FE} = [\cosh(W_B/L_n) - 1]^{-1} \quad (5)$$

For edge-coupled double-heterojunction phototransistors, if only TE modes are excited, $g(y)$ has a near $\{1-\cos(2\gamma y)\}$ dependence and G_{opt} in edge-coupled double-heterojunction phototransistors with a fully depleted collector is given by

$$G_{opt,edge} \approx A \{B(C.D) + E.F\} \quad (6)$$

where

$$A = \frac{(1 - e^{-\Gamma \alpha \Lambda})}{\Gamma(W_B + W_C)}, \quad B = (1 + h_{FE}),$$

$$C = \left[\frac{2\gamma L_n^2}{1 + 4\gamma^2 L_n^2} + \frac{1}{2\gamma} \right], \quad D = \sin(2\gamma W_B) + W_C,$$

$$E \left[\frac{\cos(2\gamma W_B)}{1 + 4\gamma^2 L_n^2} - 1 \right], F = \frac{L_n [1 + \cosh(W_B/L_n)]}{\sinh(W_B/L_n)}$$

In Eq. (6), α is the absorption coefficient in the base and collector, Γ is the fraction of optical power in the absorbing regions and Λ is the length of the waveguide. [Equation (6) corrects typographical errors in Eq. (22) of Ref. 7]. As with top-entry double heterojunction phototransistors, the term containing $(1+h_{FE})$ is dominant.

In this model, the optical gain of both top-entry and edge-coupled heterojunction phototransistor depends only on W_B , W_C and L_n . Leaving aside questions about its validity, the main uncertainty in evaluating G_{opt} from Eq. (4) or Eq. (6) lies in the value of L_n . From measurements of electron diffusion length in p-type InGaAs [13], a value of L_n in the range ~ 0.5 - $2\mu\text{m}$ seems appropriate in an optically biased edge-coupled heterojunction phototransistor.

Figures (3) and (4) compare the variation of G_{opt} with W_B for top-entry and edge-coupled double-heterojunction phototransistors calculated from Eqs. (4) and (6) with $L_n=1\mu\text{m}$, for $W_C=0.3$ and $0.4\mu\text{m}$. For both structures G_{opt} rapidly increases with decreasing W_B , as a greater fraction of the electrons injected into the base by the optical bias reach the c-b depletion layer edge. On the other hand, reducing W_C from $0.4\mu\text{m}$ to $0.3\mu\text{m}$ has little effect. Overall, the model predicts that G_{opt} is \sim three times higher in edge-coupled double heterojunction phototransistors compared with top-entry devices with the same layer structure. To summarise this section, table (1) shows a comparison between measured and predicted values of responsivity (proportional to G_{opt}) for edge-coupled and top-entry double heterojunction phototransistor reported in the literature.

Table (1) Comparison between measured and calculated responsivity R for several double heterojunction phototransistors structures reported in the literature, with $L_n = 1\mu\text{m}$

Reference	R (A/W) Measured	R (A/W) Predicted	DHPT type
1	85-175	60	Edge-coupled
3	40-100	53	Edge-coupled
6	50	40	Edge-coupled
4	10	13*	Top-entry
5	50	52	Top-entry

* The measured value of h_{FE} was used to calculate G_{opt} for this structure

4. Modelling Results

Monte Carlo calculations of electron transport were performed, to elucidate the limits on the validity of Eqs. (4) and (6). The approach used the results of a drift-diffusion model [14] to provide the initial illuminated charge distribution for the Monte Carlo simulations, with the optical power absorbed continuously and uniformly through the quasi-neutral base and c-b depletion layers. The charge distributions were allowed to relax during the Monte Carlo run subject to the integrated hole density less

the ionised acceptor density across the illuminated region remaining constant. This hybrid approach enables the omission of generation and recombination (g-r) from the Monte Carlo model, which operates on virtual time scales much faster than the g-r processes. Instead, the initial charge densities input from the drift-diffusion calculation accurately include the effect of Shockley-Read-Hall recombination.

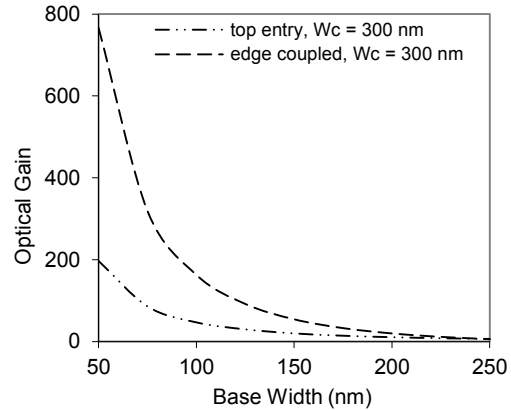


Fig. (3) Calculation of variation of G_{opt} with W_B for top-entry and edge-coupled double heterojunction phototransistors with depleted collector width of $0.3\mu\text{m}$, with $L_n=1\mu\text{m}$

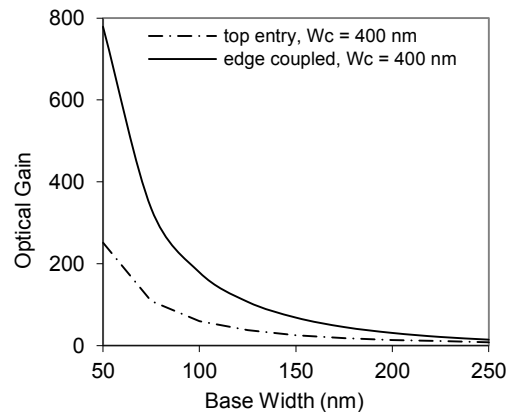


Fig. (4) Calculation of variation of G_{opt} with W_B for top-entry and edge-coupled double heterojunction phototransistors with depleted collector width of $0.4\mu\text{m}$, with $L_n=1\mu\text{m}$

The Monte-Carlo model employs three non-parabolic valleys (Γ , L and X) to simulate the conduction band structure and two spherical parabolic bands for the valence band structure. It includes scattering from acoustic phonons, polar and non-polar optical phonons and from ionised impurities. Alloy scattering was also included for the InGaAs layers [15]. The electron and hole velocity-field curves predicted by the model reproduce published data with excellent precision [16].

Figure (5) shows, for different values of V_{CE} , the variation of (a) the electron ensemble energy, (b) the electron ensemble velocity, and (c) the hole ensemble energy while figure (6) shows the electron occupancy of the Γ and L conduction valleys with

distance through the optically biased two terminal double heterojunction phototransistor detailed in Table (2). The absorbed optical power was 15 μ W.

Table (2) Details of two-terminal double heterojunction phototransistor used in Monte Carlo modelling

Layer	Material	Doping density (cm ⁻³)	Width μ m
Emitter	InP	5.1×10^{17} n	0.15
Base	InGaAs	5.1×10^{18} p	0.1
Collector	InGaAs	1.0×10^{16} n	0.4
Sub-collector	InP	1.0×10^{19} n	0.15

Except for low V_{CE} , hot electron injection into the base occurs with the ensemble energy being maintained across the base as the electrons undergo quasi-ballistic transport with very little scattering. The electron velocity increases as they traverse the base, reaching a peak value at or near the edge of the c-b depletion region. The increase arises from distortion of the velocity distribution function due to the electric field in the c-b depletion layer preventing electrons from scattering back into the base [11].

On entering the c-b depletion region, the electric field causes an increase in the electron kinetic energy, although their velocity decreases to a near-constant level from a peak value at or near the neutral base edge. The decrease originates from non-parabolicity of the Γ -valley causing an increase in effective mass as electrons gain energy and, for higher V_{CE} , significant scattering into the L valley.

These results demonstrate the need to consider the quasi-ballistic nature of carriers transiting from emitter to collector when analysing heterojunction phototransistor performance. Yet, table (1) shows that Eqs. (6) and (7) provide good estimates of the optical gain of practical double heterojunction phototransistors. This paradox is resolved by recalling that the dominant contribution to G_{opt} comes from the amplification of the primary photocurrent generated in the c-b depletion region. To a good approximation, G_{opt} given by Eqs. (4) and (6) reduces to the form

$$G_{opt} \sim K(1 + h_{FE})J_{dp} \quad (7)$$

where K and J_{dp} do not depend on the assumption of diffusive transport. Only the form of h_{FE} needs correction to obtain meaningful estimates of G_{opt} from Eqs. (4) and (6). The transistor gain can be defined in terms of the minority carrier lifetime, τ_n , and τ_b , their transit time across the base [17,18]

$$h_{FE} = \frac{\tau_n}{\tau_b} \approx \frac{2L_n^2}{W_B^2} \left[1 + \frac{2\lambda_n}{W_B} \right]^{-1} \quad (8)$$

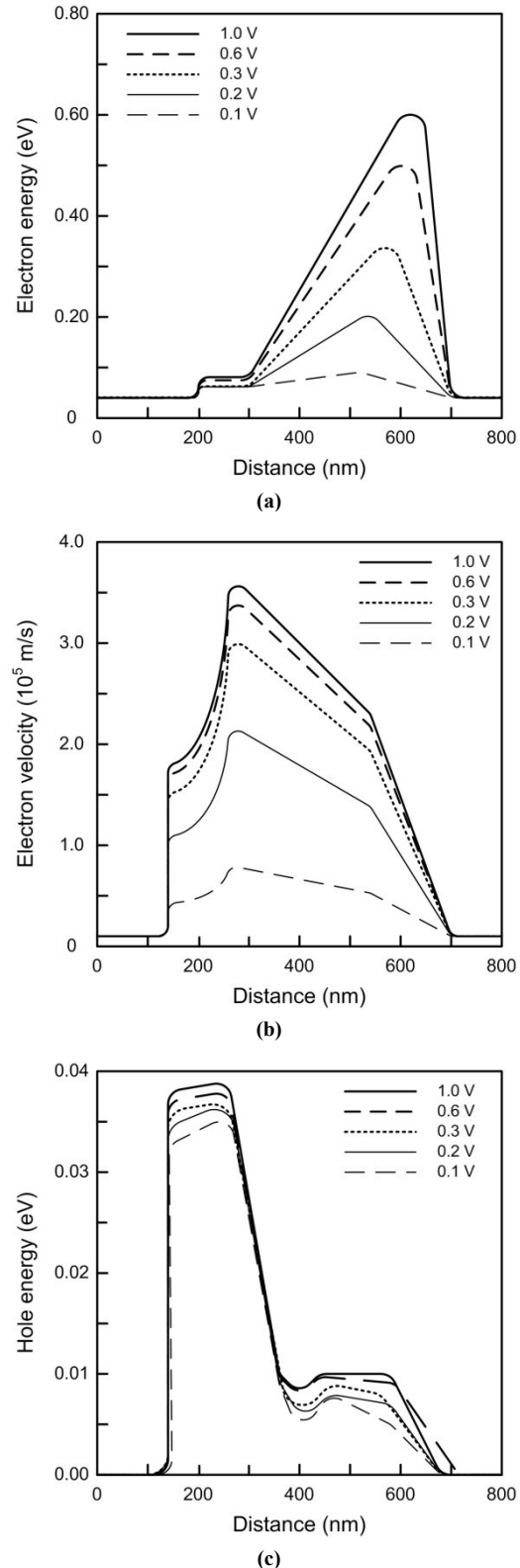


Fig. (5) Results of Monte Carlo simulation for various V_{CE} : (a) electron ensemble energy, (b) electron ensemble velocity, and (c) hole energy as functions of distance

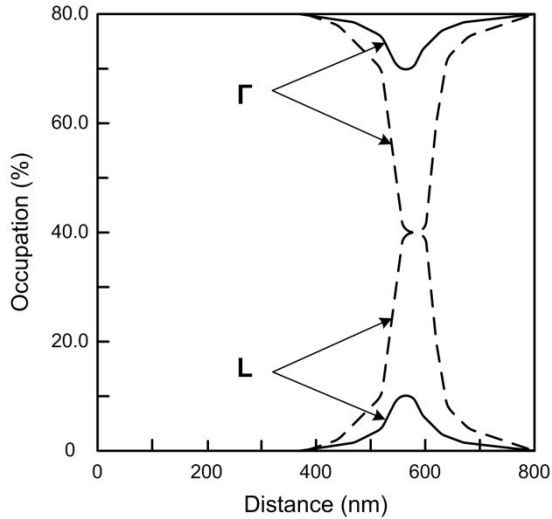


Fig. (6) Results of Monte Carlo simulation for Γ - and L- valley occupancy ($V_{CE}=0.6, 1.0$ V only) as functions of distance

The second part of Eq. (8) makes a semi-analytical correction to τ_b to account for quasi-ballistic base transport in terms of a characteristic length, λ_B , for momentum relaxation in the base [17]. Equation (8) implies that when diffusion dominates h_{FE} has the W_B^{-2} dependence given by Eq. (5) if $W_B \ll L_n$. With small W_B , h_{FE} shows a W_B^{-1} dependence characteristic of ballistic transport. Such behaviour has been observed in InAlAs/InGaAs heterojunction bipolar transistors with base doping of 1.5×10^{19} acceptors/cm³, with the crossover from diffusion like to quasi-ballistic base transport occurring for $W_B \sim 0.1 \mu\text{m}$ [19]. On the other hand, Ref. [21] reports a W_B^{-2} dependence for base widths down to $0.025 \mu\text{m}$ in InP/InGaAs heterojunction bipolar transistors with base doping of 7×10^{19} acceptors/cm³. The discrepancy can be explained by the reduction in minority carrier lifetime with increased doping level [13]. Therefore, analytic models of optical gain based on minority carrier diffusion regain first order validity by correcting the expression used for h_{FE} , or by using measured values of gain for the corresponding heterojunction bipolar transistor technology.

The cut-off frequency of conventional rf bipolar transistors can be found from the formula [10]

$$\frac{1}{2\pi f_T} = \frac{kT}{qI_E} (C_{EB} + C_{CB} + C_p) + R_C C_{TC} + \tau_b + \tau_{cb} \quad (9)$$

Figure (7) shows the variation with V_{CE} in τ_b and τ_{cb} for the two-terminal double heterojunction phototransistor detailed in Table (3), calculated via

$$\tau_b = \int_0^{W_B} \frac{dy}{v(y)} \quad \tau_{cb} = \int_{W_B}^{W_B+W_C} \left(1 - \frac{y}{W_C}\right) \frac{dy}{v(y)} \quad (10)$$

Once V_{CE} is large enough to deplete fully the narrow band gap collector layer, τ_{cb} has a near-constant value of ~ 0.35 ps, before rising to ~ 0.5 ps for $V_{CE}=1.0$ V, when substantial scattering into the L-valley occurs. This is much smaller than value of τ_{cb}

of ~ 0.9 ps obtained from the traditional expression $\tau_{cb} = X_d / (2v_s)$, reflecting the higher entry velocity of quasi-ballistic electrons into the c-b depletion layer. Similarly, τ_b drops to a near constant ~ 0.1 ps, a value much less than that obtained from the diffusion-based formula [$\tau_b = W_B^2 / (2D_n)$]. Although the corrections to τ_{cb} and τ_b are large, their combined impact on f_i is small compared to the RC time contributions.

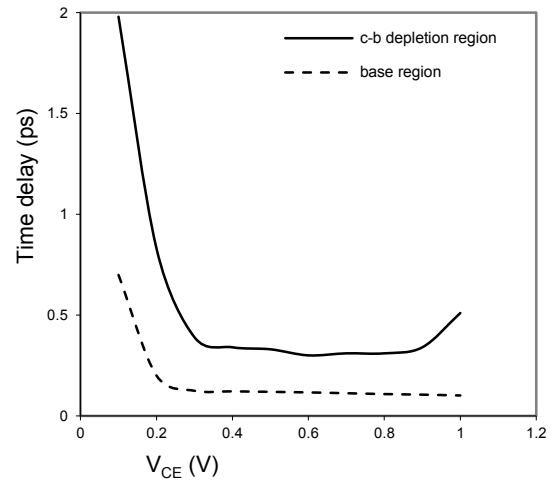


Fig. (7) Signal delay associated with quasi-ballistic electrons transiting the neutral base of the double heterojunction phototransistor

5. Conclusion

Monte Carlo simulations of transport through the base and collector-base depletion regions of an optically biased, two-terminal double heterojunction phototransistor provide new insight into the validity of simple analytical models of device performance. Whilst quasi-ballistic transport occurs in the base, it can be accounted for by using a modified expression for the common emitter gain in analytical models of optical gain. The available evidence indicates that the correction is small, even in very narrow bases, if the base doping is high ($N_B \sim 5 \times 10^{19}$ impurities/cm³). Although the corrections to the base and c-b depletion layer transit times are large, the impact on estimates of f_i by simple theory is small owing to the dominance of RC time constants.

REFERENCES

- [1] D. Wake, D.J. Newson, M.J. Harlow and I.D. Henning, "Optically biased, edge-coupled InP/InGaAs heterojunction phototransistors", *Electron. Lett.*, 29 (1993) 2217-2218.
- [2] J. Van de Castelee, J.P. Vilcot, J.P. Gouy, F. Mollot and D. Decoster, "Electro-optical mixing in an edge-coupled GaInAs/InP heterojunction phototransistor", *Electron. Lett.*, 32 (1996) 1030-1032.
- [3] C.P. Liu, A.J. Seeds and D. Wake, "Two-terminal edge-coupled InP/InGaAs heterojunction

phototransistor optoelectronic mixer”, *IEEE Microwave and Guided Wave Lett.*, 7 (1997) 72-74.

[4] M. Muller, M. Riet, J.L. Benchimol, C. Fortin and C. Gonzalez, “28 and 42 GHz narrow-band InP based phototransistor mixers for hybrid fibre radio distribution systems,” in *Proc. 9th IEEE Int. Workshop on High Performance Electron Devices for Microwave and Optoelectronic Applications*, Vienna, 2001, pp. 249-254.

[5] H. Kamitsuna, Y. Matsuoka, S. Yamahata and N. Shigekawa, “Ultra-high speed InP/InGaAs DHPTs for OEMMICs,” *IEEE Trans. Microwave Theory Tech.*, 39 (2001) 1921-1925.

[6] V. Magnin, J. Van de Castele, J.P. Vilcot, J. Harari, J.P. Gouy and D. Decoster, “A three terminal edge-coupled InGaAs/InP heterojunction phototransistor for multifunction operation,” *Microwave Opt. Technol. Lett.*, 17 (1998) 408-412.

[7] D.W.E. Allsopp, M.S. Stern, E. Strobel, “Analysis of edge-coupled heterojunction phototransistors,” *IEEE Trans. Microwave Theory Tech.*, 47 (1999) 1289-1296.

[8] M.S. Stern, “Semivectorial polarised finite difference method for optical waveguides with arbitrary index profiles”, *IEE Proc. J Optoelectron.*, 135 (1988) 56-63.

[9] J.C. Campbell, “Phototransistors for lightwave communications”, *Semiconductors and Semimetals, Lightwave Communications Technology*, 22, part D, Orlando, Florida: Academic Press, 1985, pp. 389-447.

[10] H.F. Cooke, “Microwave Transistors: Theory and Design”, *Proc. IEEE*, 59 (1971) 1163-1181.

[11] R.J. Mills, D.C. Herbert, J.H. Jefferson and A.B. Walker, “Monte Carlo calculations of base transit

time in bipolar transistors”, *Semicond. Sci. and Technol.*, 8 (1993) 1719-1723.

[12] N. Chand, P.A. Houston, P.N. Robson, “Gain of a heterojunction bipolar phototransistor,” *IEEE. Trans. Electron Dev.*, ED-32 (1985) 622-627.

[13] P. Ambrée, B. Gruska and K. Wandel, “Dependence of electron diffusion length in p-InGaAs layers on the acceptor diffusion process”, *Semicond. Sci. Technol.*, 7 (1992) 858-860.

[14] S.J. Woods, A.B. Walker and D. Wake, “Simulation of optically biased edge coupled InP/InGaAs phototransistors”, in *Proc. 5th IEEE Int. Workshop on High Performance Electron Devices for Microwave and Optoelectronic Applications*, London, 1997, pp. 205-210.

[15] M.A. Littlejohn, J.R. Hauser, T.H. Glisson, D.K. Ferry and J.W. Harrison, “alloy scattering and high field transport in ternary and quaternary III-V semiconductors (FET model)”, *Solid State Electron.*, 21 (1978) 107-114.

[16] J.H. Marsh, “Effects of compositional clustering on electron transport in $\text{In}_{0.53}\text{Ga}_{0.47}\text{As}$ ”, *Appl. Phys. Lett.*, 41 (1982) 732-734.

[17] D.C. Herbert, “Quasi-ballistic corrections to base transit time in bipolar transistors”, *Semicond. Sci. Technol.*, 6 (1991) 405-407.

[18] D. Ritter, R.A. Hamm, A. Feyngenson, M.B. Panish and S. Chandrasekhar, “Diffusive base transport in narrow base In/Ga_{0.47}In_{0.53}As heterojunction bipolar transistors”, *Appl. Phys. Lett.*, 59 (1991) 3431-3433.

[19] A.F.J. Levi, B. Jalali, R.N. Nottenburg, A.Y. Cho, “Vertical scaling in heterojunction bipolar transistors with non-equilibrium base transport”, *Appl. Phys. Lett.*, 60 (1992) 460-4462.